ORIGINAL PAPER

CRYSTAL Research & Technology

www.crt-journal.org

Growth and Properties of Intentionally Carbon-Doped GaN Layers

Eberhard Richter, Franziska C. Beyer, Friederike Zimmermann, Günter Gärtner, Klaus Irmscher, Ivan Gamov, Johannes Heitmann, Markus Weyers, and Günther Tränkle*

Carbon-doping of GaN layers with thickness in the mm-range is performed by hydride vapor phase epitaxy. Characterization by optical and electrical measurements reveals semi-insulating behavior with a maximum of specific resistivity of 2×10^{10} Ω cm at room temperature found for a carbon concentration of 8.8×10^{18} cm^{-3}. For higher carbon levels up to 3.5×10^{19} cm^{-3}, a slight increase of the conductivity is observed and related to self-compensation and passivation of the acceptor. The acceptor can be identified as C_N with an electrical activation energy of 0.94 eV and partial passivation by interstitial hydrogen. In addition, two differently oriented tri-carbon defects, C_N-a-C_{Ga}-a-C_N and C_N-a-C_{Ga}-c-C_N, are identified which probably compensate about two-thirds of the carbon which is incorporated in excess of 2×10^{18} cm^{-3}.

1. Introduction

Gallium nitride is a semiconductor commercialized in light-emitting devices and used in upcoming microwave and power devices.[1] Especially in the latter, carbon as impurity or as intentional dopant plays an important role for the device performance and reliability. Carbon is incorporated as an impurity due to the metalorganic sources in metalorganic vapor phase epitaxy (MOVPE) which is often employed for the growth of device layer structures.[2] Its control is crucial for layers with low doping levels and nonuniform incorporation of carbon can reduce the breakdown voltage of electronic devices dramatically.[3–6] Carbon is suspicious to be related to current collapse and dispersion in transistors when used intentionally in highly resistive buffer layers.[7,8] Thus, the electronic properties of carbon in GaN remain of high interest. Hydride vapor phase epitaxy (HVPE) and molecular beam epitaxy (MBE) are techniques which are inherently carbon-free and carbon incorporation is therefore minimized. They allow for the investigation of intentional carbon doping without interference from unintentionally incorporated carbon. Doping of GaN with propane in HVPE revealed that carbon together with oxygen and hydrogen results in at least two transitions of yellow defect luminescence (YL) with a deep acceptor involved.[9] An investigation in rf plasma-assisted MBE with CBr_4 as carbon source revealed that carbon in concentrations up to 10^{19} cm^{-3} has no negative influence on structural properties of GaN but compensates Si donors.[10] Ab initio DFT calculations and comparison with experimental data from carbon doping in MOVPE suggested the occupation of a nitrogen place by carbon C_N being an acceptor as energetically most probable for an excess of donors but self-compensation due to uptake of carbon on gallium sites C_{Ga} or as interstitials C_i would be also probable.[11] Most of these early findings while still valid in principle have been refined in the last decade. Today, there is consensus that C_N forms a deep acceptor with an electrical activation energy of about 0.9 eV and recently p-type conductivity at temperatures above 350 °C in C-doped GaN grown by HVPE with methane as doping source was reported.[12,13] The origin of the blue luminescence (BL2) at 3 eV is assigned to an interstitial hydrogen atom H_i bond to C_N or an O_NC_N complex and the yellow luminescence YL at 2.25 eV to the C_N or O_NC_N itself.[14,15] However, theoretical predictions assume O_NC_N as energetically less favorable and even C_i as rather improbable under most experimental conditions, whereas C_N and C_N-H_i should form a deep acceptor and a neutral center (hydrogen passivated C_N) and are responsible for YL and BL2.[16]

Dr. E. Richter, Prof. M. Weyers, Prof. G. Tränkle
Ferdinand-Braun-Institut
Leibniz-Institut für Höchstfrequenztechnik
Gustav-Kirchhoff-Str. 4, 12489 Berlin, Germany
E-mail: eberhard.richter@fbh-berlin.de

Dr. F. C. Beyer, F. Zimmermann, Prof. J. Heitmann
Institute of Applied Physics
TU Bergakademie Freiberg
09599 Freiberg, Germany

Dr. G. Gärtner
Institute of Experimental Physics
TU Bergakademie Freiberg
09599 Freiberg, Germany

Dr. K. Irmscher, I. Gamov
Leibniz-Institut für Kristallzüchtung
Max-Born-Strasse 2, 12489 Berlin, Germany

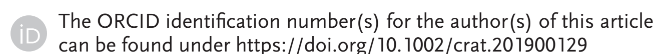
The ORCID identification number(s) for the author(s) of this article can be found under https://doi.org/10.1002/crat.201900129

© 2019 The Authors. Published by WILEY-VCH Verlag GmbH & Co. KGaA, Weinheim. This is an open access article under the terms of the Creative Commons Attribution-NonCommercial-NoDerivs License, which permits use and distribution in any medium, provided the original work is properly cited, the use is non-commercial and no modifications or adaptations are made.

The copyright line for this article was changed on 25 October 2019 after original online publication.

DOI: 10.1002/crat.201900129

Carbon on Ga site C_{Ga} is predicted under N-rich growth conditions for the case that the Fermi level is below 2 eV.[16] This could occur in vapor phase epitaxy or N-rich MBE due to Fermi level pinning at 0.9 eV in case of high acceptor concentrations, for example, after incorporation of a sufficiently high level of C_N. C_{Ga} is predicted to be a shallow donor and therefore is a candidate for self-compensation. The discussion about the details of these models and the conclusions has not been finished yet and parts of the picture of incorporation of carbon and its role in GaN are still incomplete and become more important again with improving material quality and new applications. Thus, new theoretical investigations include not only single carbon configurations C_N, C_{Ga}, and C_i but also complexes between them.[12] C_N-C_{Ga} complexes were predicted to occur with a bond parallel to the c-axis (C_N-c-C_{Ga}) and with a bond nearly perpendicular to the c-axis (C_N-a-C_{Ga}) with similar formation energies and a neutral charge state for $E_F > 0.52$ eV. Traps related to carbon and its complexes are discussed and vibrational frequencies for possible C_i, C_i-C_N, and C_i-C_{Ga} are given.[12] Furthermore, complexes of carbon with oxygen, hydrogen, and silicon are discussed and their vibrational frequencies are predicted by Matsubara and Bellotti.[17] Carbon incorporation takes places at the growing surface. Thus, it will be governed by surface states and associated with this by the position of the Fermi level at the surface. There are some theoretical studies on surface states of nitride surfaces and also a recent paper on the impact of the surface structure on carbon incorporation.[18–20] However, the latter study is limited to potential incorporation sites for a single C atom. In this work, thick GaN layers were grown by HVPE and intentionally doped with carbon with the objective to identify the occupation site of carbon or its complexes experimentally. We have only studied the final balance of C_N and C_N-C_{Ga}-C_N complexes and their configuration in the bulk. Since we have not performed extensive parameter studies, no conclusion on the mechanism leading to the formation of the C_N-C_{Ga}-C_N complexes can be drawn except for the trivial statement that the probability for formation of such complexes increases with increasing C uptake. Two vibrational modes were found which are similar to the one of the tri-carbon-defect found previously in AlN.[21] Experimental evidence is given for the existence of two configurations of tri-carbon defects in GaN involving C_{Ga} which occur at a significant level and are candidates for the observed self-compensation during C doping of GaN.

2. Experimental Section

The growth of GaN layers by hydride vapor phase epitaxy (HVPE) was performed on templates grown by metalorganic vapor phase epitaxy consisting of 3.8 µm thick GaN layers on (0001) oriented sapphire substrates of 2 in. in diameter with a 0.2° miscut toward $(1\bar{1}00)$. The HVPE growth process was the same as described before with additional injection of pentane as doping source.[22] Liquid pentane (electronic grade, Dockweiler Chemicals) in a bubbler has been attached like a conventional metalorganic doping source to the gas mixing system and was transported by hydrogen as carrier gas. A vapor pressure of 308 hPa was calculated at 5 °C. Amounts of 8, 17, 69, 181, 272, 576, and 1033 µmol min^{-1} pentane were injected into the group III precursor stream in the reactor after the formation of GaCl from metallic Ga and HCl but before mixing with the group V source ammonia at the substrate surface. Thus, the III/IV ratio is constant at the reaction front which results in laterally uniform doping of the GaN layer. Finally, for some experiments, the pentane bubbler was substituted by two connected butane gas cylinders, one isotopically enriched with ^{13}C (Sigma Aldrich, Butane 13C4 (Gas) 99%), the other with the natural isotopic abundance of carbon (Butane 12C4 (Gas) 99%). Each cylinder had a volume of 0.5 l and an initial pressure of about 1500 hPa. The decreasing pressure during operation was measured by the pressure controller of the doping line and the input flow rate by the injection mass flow controller. In this way, the carbon-doping from butane was established and a GaN layer doped with ^{13}C was realized. Ga crucible and gas inlets were made from pBN to minimize Si incorporation with background Si levels below 10^{16} cm^{-3}. Each layer was grown in the same sequence as follows: A non-intentionally doped GaN layer was grown at a rate of about 450 µm h^{-1} at 990 °C for 30 min (225 µm) followed by a temperature ramp over 5 min and growth of the C-doped GaN layer at a rate of about 400 µm h^{-1} at 1010 °C for 150 min resulting in a layer thickness of 1 mm. The growth was prolonged in one case for 10 h to achieve a 4 mm thick crystal from which an a-plane oriented sample was cut out with a wire saw. All layers separated from the sapphire substrates spontaneously after cool-down due to the large difference of the thermal expansion coefficients. Samples were diced and polished to remove the initial n.i.d. GaN layer completely. Finally, subsurface damage was removed by ICP etching of about 7 µm at each side. This yielded c-plane oriented samples of 10 mm × 5 mm × 0.5–1 mm and of 8 mm × 8 mm × 0.5–1 mm for optical and electrical measurements. The size of the a-plane sample was 5 mm × 4 mm × 0.3 mm. Secondary ion mass spectrometry (SIMS) was performed for [^{12}C], [^{13}C], [O], [H], and [Si].[23] X-ray rocking curves were recorded as omega-scans with an open detector using an X'Pert Pro from Malvern Panalytical at the reflection planes (0002) and $(30\bar{3}2)$, called 002 and 302 reflections in the following. A panchromatic cathodoluminescence plan-view image was used to determine the threading dislocation density quantitatively. 2θ scans were performed in triple-axis geometry at the 004 and 006 reflections to determine the lattice constant c and at the reflections 105, 106, 204, and 205 to determine the lattice constant a according to the Fewster method.[24,25] The residual strain in the free-standing GaN layers was estimated using the lattice constants $c_0 = 0.518523$ nm and $a_0 = 0.318926$ nm.[26] At the corners of the squared samples, V/Al/Ni/Au contacts with a size of 0.8 mm × 0.8 mm were prepared and subsequently annealed with RTA at 380 °C for 3 min. Conductivity and Hall effect measurements up to 500 °C were performed using a Keithley K925B system and a Lakeshore temperature stage. Photoluminescence (PL) investigations were performed at 20 K in the wavelength range from 340 to 1100 nm using a 325 nm HeCd laser with an excitation power density of about 0.85 W cm^{-2}, a 0.5 m grating monochromator, and a Si-CCD detector. All spectra were corrected for the spectral response of the PL setup. UV illumination was realized by continuous exposure with the exciting laser in order to discriminate between different defects involved in the PL. Fourier-transform infrared (FTIR) absorption measurements over a large range at 80 K were performed with spectrometers Bruker Tensor 27 (7500–370 cm^{-1} with maximum

© 2019 The Authors. Published by WILEY-VCH Verlag GmbH & Co. KGaA, Weinheim

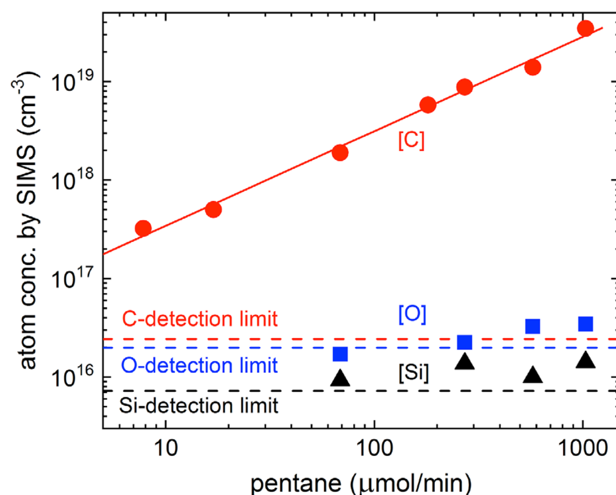

Figure 1. Concentrations of carbon, oxygen, and silicon in C-doped GaN layers measured by SIMS versus the input mole fraction of pentane.

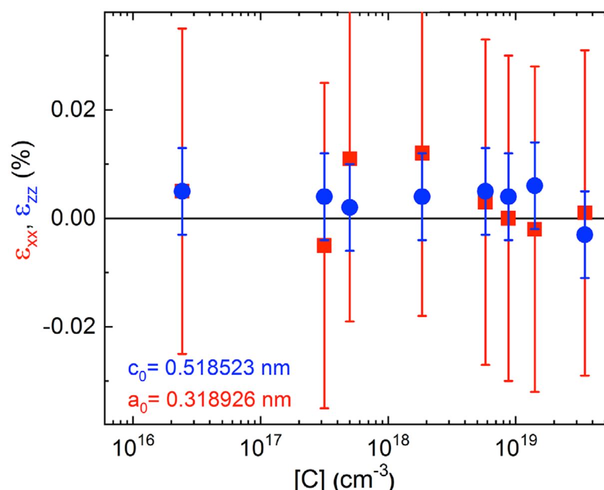

Figure 2. In-plane and out-of-plane strain ε_{xx} and ε_{zz} of the c-plane GaN layers without carbon doping (at the detection limit of 2.3×10^{16} cm^{-3}) and with carbon doping from pentane determined by X-ray diffraction. Reference lattice constants are taken from Darakchieva et al.[26]

resolution of 1 cm^{-1}) with a resolution of 2 cm^{-1}. Additional FTIR measurements were performed with a Bruker vertex 80v in the range of 1600–1800 cm^{-1} with 0.5 cm^{-1} resolution at room temperature. Polarization dependent measurements were performed with a holographic wire grid polarizer on a KRS-5 substrate and a HgCdTe detector.

3. Results and Discussion

The GaN layers were all transparent and appeared colorless for non-doped, light-grey for the lowest carbon concentration, and increasingly green with increasing carbon uptake. The background impurities C, O, and Si in the non-doped GaN layer were found to be below the detection limits (**Figure 1**) of the used SIMS. In the case of the GaN layers doped from pentane, oxygen, and silicon could be detected slightly above the detection limits (Figure 1) and hence it is assumed that traces of Si and O were introduced from the pentane source. Hydrogen is at a level of 1×10^{17} cm^{-3} for non-doped GaN layers and was found to increase to 6×10^{17} cm^{-3} for [C] of 8.8×10^{18} cm^{-3} and to 8×10^{17} cm^{-3} for [C] of 3.5×10^{19} cm^{-3}. The carbon concentration increased proportional to the pentane supply and a maximum uptake of 3.5×10^{19} cm^{-3} was achieved (Figure 1).

In **Figure 2**, it can be seen that the lattice constants are unchanged over the entire doping range and the layers have no or only very little strain. The FWHM of X-ray rocking curves for the reflections 002 and 302 of the non-doped GaN layer and the various C-doped GaN layers are compared in **Figure 3**. The FWHM at 002 is typically lower than the one at 302 in all of our non-doped GaN layers. Interestingly, this is opposite for all of our C-doped GaN layers which may support the findings of Sang et al.[5] In our case, minimum values of the FWHM of both reflections were observed for a carbon concentration around 2×10^{18} cm^{-3} with similar FWHM in 002 and lower FWHM in 302 reflection. Above this carbon concentration, a slow but continuous increase of the FWHM with carbon uptake is observed for both reflections. It is worth mentioning that the FWHMs of the used GaN/sapphire template are larger, that is, typically around 250 arcsec for the 002 reflection and around 350 arcsec for the 302 reflection. Hence, using the FWHM as a measure of crystal quality, the crystal quality of the HVPE-grown GaN layers was found to be improved in comparison to the starting MOVPE-grown GaN layer for all carbon doping levels. At [C] of about 10^{18} cm^{-3}, the FWHMs are equal or narrower compared to the non-doped GaN layer. In terms of density of the threading dislocations (TDD), it can be estimated from the FWHM, that the TDD is reduced by one order of magnitude over 1 mm GaN layer thickness.[27] Counting the dark spot density in cathodoluminescence images of the non-doped sample, a threading dislocation density of 1×10^{7} cm^{-2} was determined (**Figure 4**).

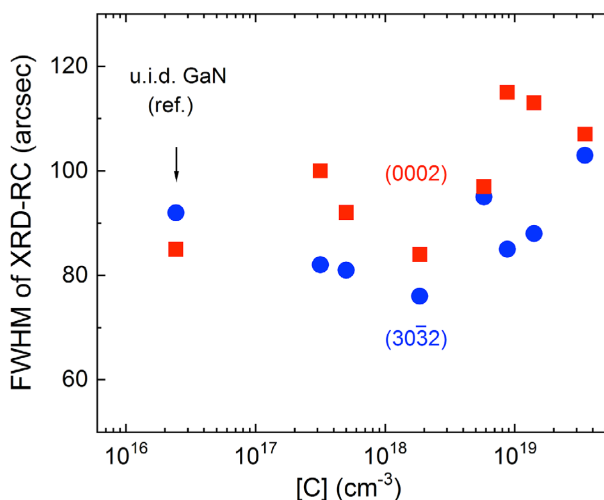

Figure 3. Full width at half maximum (FWHM) of X-ray diffraction rocking curves at the symmetric 002 reflection at the (0002) plane and the skew-symmetric 302 reflection at the (30$\bar{3}$2) plane. Note the minimum of FWHM for both reflections is not found for the non-doped layer but for the one doped with 2×10^{18} cm^{-3} carbon.

© 2019 The Authors. Published by WILEY-VCH Verlag GmbH & Co. KGaA, Weinheim

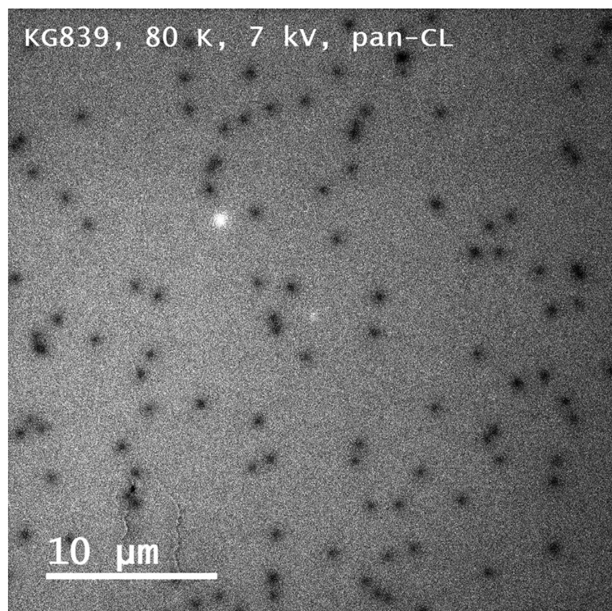

Figure 4. Cathodoluminescence micrograph recorded at the surface of the non-doped GaN layer with dark spots revealing a threading dislocation density of 1×10^{7} cm^{-2}.

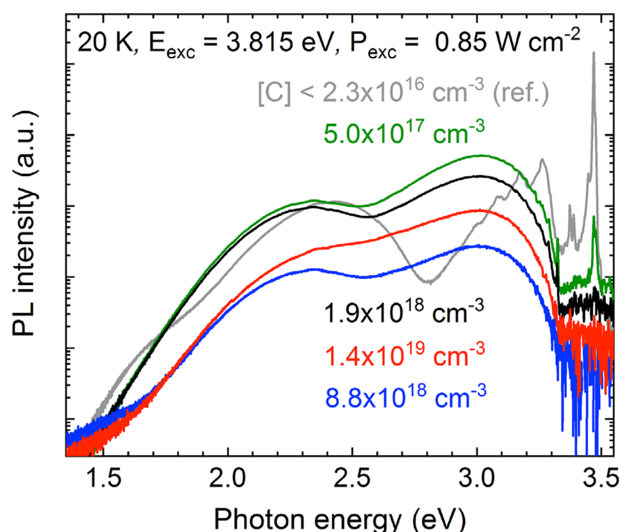

Figure 5. Photoluminescence spectra of the non-doped and C-doped GaN layers of this work.

It can be stated that the carbon doping of the samples in this work had no impact on the lattice constants of GaN and did not deteriorate the structural quality of the GaN layers. In contrast, it seems that moderate carbon doping may even improve the crystalline quality probably by stronger reduction of the edge dislocation density compared to the non-doped case.

In **Figure 5**, the photoluminescence spectra of the different samples including the non-doped GaN layer are shown. In case of the non-doped layer, near-band-edge (NBE) luminescence such as distinct transitions due to excitons, transitions from two-electron satellites, and DAP transitions can be observed as discussed already in detail by Freitas et al. for a similar non-doped GaN layer.[28] In addition, green defect luminescence around 2.4 eV can be observed which is discussed by Reshchikov et al. as a typical GL1 feature of non-intentionally doped HVPE-grown GaN layers.[15] Its origin is still under discussion.[29] In the C-doped GaN layers, the defect luminescence changes and is dominated by a blue BL2 band at 3.0 eV and yellow band at 2.25 eV called YL1 according to Reshchikov et al.[15] If this assignment is correct, then in typical carbon-doped GaN, a change of the intensities between the YL1 and BL2 should be observable in case of UV illumination due to the dissociation of C_N-H_i.[15] The NBE luminescence in the carbon-doped GaN layers is strongly decreased for the lowest intentional carbon doping of 10^{17} cm^{-3} and vanishes completely for the higher carbon doping levels. This observation agrees with earlier reports for semi-insulating GaN.[10] As shown in **Figure 6**, the expected bleaching behavior of the BL2 could be observed for illumination with UV light for 30 min. The YL1 band increased reversibly on cost of the BL2 due to the dissociation of hydrogen from C_N as expected. The semi-insulating electrical behavior could be verified by conductivity measurements as shown in **Figure 7**.

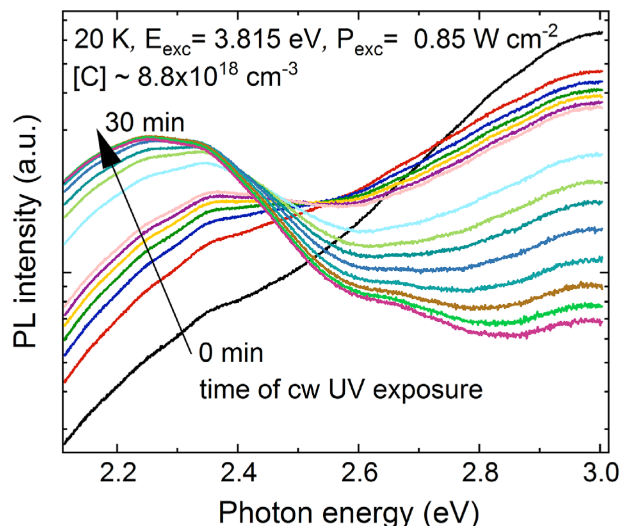

Figure 6. Photoluminescence spectrum of the defect luminescence of a C-doped GaN layer and its evolution during 30 min of UV illumination.

The Hall-effect measurements were complicated by changing signs of the Hall constant during the measurement indicating highly compensated material with low carrier mobility. Therefore, in contrast to the doping with Fe which traps electrons,[22] no serious statement about the charge carrier density and the resulting charge carrier type was possible here. That means, however, that a part of the electrical active carbon or a directly related defect is incorporated as an acceptor and another part or a directly related defect of approximately the same amount must be incorporated as a donor with a similar activation energy. The observation cannot be explained by passivation of C_N acceptors by hydrogen because the hydrogen concentration was found to be less than 10% of the carbon concentration. Interestingly, the resistivity does not increase continuously with the carbon concentration but seems to have a maximum below 1×10^{19} cm^{-3}, that is, the ratio of acceptors and donors seems not be constant but depends on the carbon concentration. The activation energy of

© 2019 The Authors. Published by WILEY-VCH Verlag GmbH & Co. KGaA, Weinheim

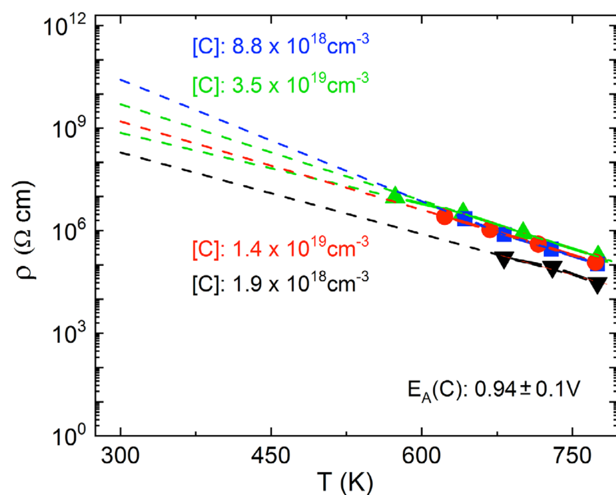

Figure 7. Temperature-dependent measurements of resistivity for C-doped GaN samples with carbon concentrations between 1.9×10^{18} cm^{-3} and 3.5×10^{19} cm^{-3}.

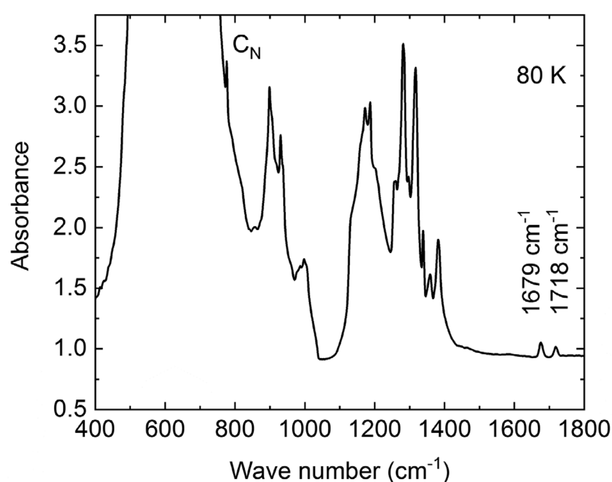

Figure 8. FTIR absorption spectrum recorded at 80 K for the GaN sample with a carbon concentration of 8.8×10^{18} cm^{-3}.

the acceptor was determined from the temperature dependence of the resistivity to 0.94+/−0.1 eV (Figure 7). The extrapolated maximum of the specific resistivity at room temperature is 2×10^{10} Ω cm.

An FTIR absorption measurement at 80 K over a wide frequency range is depicted in **Figure 8**. The broad high signal in the range from about 450 to 800 cm^{-1} is assigned to one-phonon absorption. On its high-energy flank, a narrow peak at 777.5 cm^{-1} can be seen which was already assigned as the local vibrational mode (LVM) of the substitutional carbon acceptor C_N on nitrogen site.[30] A next broad band from 1100 to 1400 cm^{-1} can be assigned to combination absorption. But then, at 1679 cm^{-1} and at 1718 cm^{-1}, two additional peaks occur which are similar to the LVM of the tri-carbon defect found in AlN.[21]

These two peaks at 1679 and 1718 cm^{-1} were investigated in more detail. It was found that they increase in intensity with the concentration of carbon and it could be estimated that these defects occur with a density of the same order of magnitude like

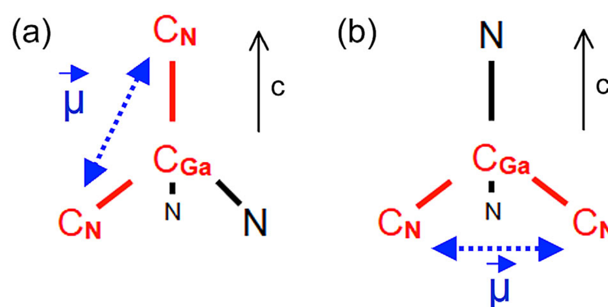

Figure 9. The axial tri-carbon defect C_N-a-C_{Ga}-c-C_N with the LVM at 1718 cm^{-1} (a) and the basal tri-carbon defect C_N-a-C_{Ga}-a-C_N with the LVM at 1679 cm^{-1} (b) are shown schematically with indication of the electric dipole moments μ of the anti-symmetric stretching modes.

the overall carbon concentration measured by SIMS.[31] Polarization dependent FTIR measurements allowed to distinguish the two tri-carbon defects illustrated in **Figure 9** crystallographically. The axial defect C_N-a-C_{Ga}-c-C_N which contains a C_{Ga}-C_N bond parallel to the *c*-axis shows a maximum of absorption for the E-vector oscillating parallel to the *c*-axis whereas the basal defect C_N-a-C_{Ga}-a-C_N which contains only bonds nearly perpendicular to *c*-axis shows its maximum of absorption for the E-vector oscillating perpendicular to the *c*-axis.[31] By rotating the polarizations by 90°, the LVM intensity of the axial defect configuration attains a minimum of one-fourth of the maximum, while that of the basal defect configuration vanishes. This is understandable from the directions of the electric dipole moments (shown in Figure 9) characterizing the anti-symmetric stretching modes of both tri-carbon defect configurations (note: the directions of the electric dipole moments do not coincide with bond directions).

Finally, *c*-plane samples doped with the ^{13}C isotope were prepared because a change of the mass changes the oscillator frequency and therefore should shift the position of the LVM absorption lines. The frequency reduction expected for a complete

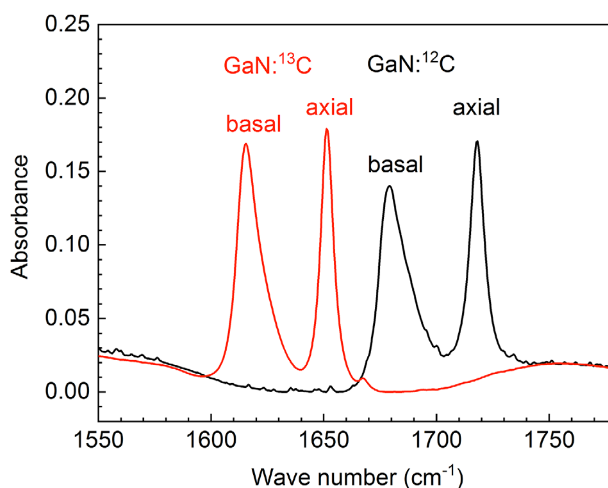

Figure 10. FTIR absorption spectra recorded at room temperature from two GaN layers doped only by ^{12}C with the LVMs at 1679 and 1718 cm^{-1} and doped only by ^{13}C with shifted LVMs to 1615 and 1651 cm^{-1}.

© 2019 The Authors. Published by WILEY-VCH Verlag GmbH & Co. KGaA, Weinheim

exchange of the ^{12}C atoms by ^{13}C by a factor of $(12/13)^{1/2} = 0.96$ is in full agreement with the observed shifts of the two LVMs from 1679 to 1615 cm^{-1} and from 1718 to 1651 cm^{-1}, respectively, as shown in **Figure 10**. This strongly supports the made assignments for the found defects.

4. Conclusions

GaN layers were grown by HVPE and doped with carbon using either pentane or, for layers intentionally doped with the isotope ^{13}C, butane. Carbon concentrations up to 3.5×10^{19} cm^{-3} were realized and no detrimental impact on structural properties could be found. Photoluminescence revealed signatures which are quite characteristic for carbon-doped GaN of high quality. Bleaching of the BL2 under UV light was assigned to dissociation of interstitial hydrogen bound to carbon substitutionally incorporated on nitrogen site C_N. The substitutional incorporation on nitrogen sites C_N was verified and here carbon acts as an acceptor. Passivation of C_N by hydrogen takes place but was limited here to below 10% of the overall carbon concentration. The C-doped GaN layers were found to be highly resistive with a maximum specific resistivity of 2×10^{10} Ω cm at room temperature for a carbon doping of nearly 10^{19} cm^{-3}. For carbon concentration above 2×10^{18} cm^{-3} the onset of self-compensation was observed which is accompanied by appearance of additional features in FTIR absorption at 1679 and 1718 cm^{-1}. These can be assigned to the two tri-carbon defects C_N-a-C_{Ga}-c-C_N oriented parallel to the *c*-axis and C_N-a-C_{Ga}-a-C_N perpendicular to the *c*-axis. Donors in form of carbon atoms substitutionally incorporated on gallium sites C_{Ga} are assumed to be a reason for self-compensation. The two tri-carbon-defects form with a density that makes them candidates to explain the observed self-compensation at high carbon incorporation. It is known that the incorporation of carbon strongly depends on growth conditions. Therefore, it is interesting to note that the characteristic LVMs of the described tri-carbon-defects had already been seen before in GaN layers with high carbon content without their origin being identified. Hao et al. observed these LVMs already in 1999 in carbon-rich GaN grown by sublimation.[32] Ito et al. observed these LVMs in MOVPE-grown GaN layers in case of intentional carbon doping and already suspected a relation to the carbon dopant.[26] Therefore, there is no doubt that the findings here are applicable to carbon-doped GaN layers grown by other techniques. The findings indicate that doping with carbon for devices can be delicate. Recent findings even show that the intrinsic incorporation of carbon in GaN may not be stable and changes of lattice places from C_N to C_{Ga} may take place even at growth temperatures.[33] From the complexity of the role of carbon in GaN, one may conclude that iron could be the generally better choice to achieve semi-insulating behavior in GaN, because it is incorporated at a unique lattice site as Fe_{Ga} being an acceptor about 0.6 eV below the conduction band.[28] However, also iron has its challenges because diffusion of iron from iron-doped GaN to non-doped GaN layers during MOVPE was observed.[34] Thus, the right choice of the dopant may strongly depend on the application and the right choice of growth procedure. The above findings are also of technological importance because they provide guidelines for optimization of intentionally carbon-doped semi-insulating GaN layers.

Acknowledgements

E. R. likes to thank Mr. Thomas Tessaro for technical assistance in the realization of carbon doping with ^{12}C and ^{13}C from butane and the German branch of Sigma Aldrich for their supply of the butane sources.

Conflict of Interest

The authors declare no conflict of interest.

Keywords

carbon, GaN, HVPE, self-compensation, tri-carbon-defect

Received: July 1, 2019
Revised: August 21, 2019
Published online: October 22, 2019

[1] a) https://www.nobelprize.org/uploads/2018/06/press-25.pdf (accessed: May 2019); b) http://www.semiconductor-today.com/news_items/2019/jan/yole_030119.shtml (accessed: May 2019); c) Yole Développement, *RF GaN Market: Applications, Players, Technology and Substrates 2019*, Market & Technology Report, May **2019**.
[2] D. D. Koleske, A. E. Wickenden, R. L. Henry, M. E. Twigg, *J. Cryst. Growth* **2002**, *242*, 55.
[3] T. Tanaka, N. Kaneda, T. Mishima, Y. Kihara, T. Aoki, K. Shiojima, *Jpn. J. Appl. Phys.* **2015**, *54*, 041002.
[4] F. Kaess, S. Mita, J. Xie, P. Reddy, A. Klump, L. H. Hernandez-Balderrama, S. Washiyama, A. Franke, R. Kirste, A. Hoffmann, R. Collazo, Z. Sitar, *J. Appl. Phys.* **2016**, *120*, 105701.
[5] L. Sang, B. Ren, M. Sumiya, M. Liao, Y. Koide, A. Tanaka, Y. Cho, Y. Harada, T. Nabatame, T. Sekiguchi, S. Usami, Y. Honda, H. Amano, *Appl. Phys. Lett.* **2017**, *111*, 122102.
[6] H. Fujikura, K. Hayashi, F. Horikiri, Y. Narita, T. Konno, T. Yoshida, H. Ohta, T. Mishima, *Appl. Phys. Express* **2018**, *11*, 045502.
[7] B. Klein, S. C. Binari, K. Ikossi, A. E. Wickenden, D. D. Koleske, R. L. Henry, *Appl. Phys. Lett.* **2001**, *79*, 3527.
[8] C. Koller, G. Pobegen, C. Ostermaier, D. Pogany, in *Proc. of the Int. Electron Devices Meeting (IEDM)*, IEEE, Piscataway, NJ **2017**, pp. 33.4.1–33.4.4.
[9] R. Zhang, T. F. Kuech, *Mater. Res. Soc. Symp. Proc.* **1998**, *482*, 709.
[10] D. S. Green, U. K. Mishra, J. S. Speck, *J. Appl. Phys.* **2004**, *95*, 8456.
[11] C. H. Seager, A. F. Wright, J. Yu, W. Götz, *J. Appl. Phys.* **2002**, *92*, 6553.
[12] M. Matsubara, E. Bellotti, *J. Appl. Phys.* **2017**, *121*, 195701.
[13] M. Iwinska, R. Piotrzkowski, E. Litwin-Staszewska, T. Sochacki, M. Amilusik, M. Fijalkowski, B. Lucznik, M. Bockowski, *Appl. Phys. Express* **2017**, *10*, 011003.
[14] D. O. Demchenko, I. C. Diallo, M. A. Reshchikov, *J. Appl. Phys.* **2016**, *119*, 035702.
[15] M. A. Reshchikov, M. Vorobiov, D. O. Demchenko, Ü. Özgür, H. Morkoç, A. Lesnik, M. P. Hoffmann, F. Hörich, A. Dadgar, A. Strittmatter, *Phys. Rev. B* **2018**, *98*, 125207.
[16] J. L. Lyons, A. Janotti, C. G. Van der Walle, *Phys. Rev. B* **2014**, *89*, 035204.
[17] M. Matsubara, E. Bellotti, *J. Appl. Phys.* **2017**, *121*, 195702.
[18] C. G. V. de Walle, D. Segev, *J. Appl. Phys.* **2007**, *101*, 081704.
[19] P. Reddy, I. Bryan, Z. Bryan, W. Guo, L. Hussey, R. Collazo, Z. Sitar, *J. Appl. Phys.* **2014**, *116*, 123701.
[20] P. Kempisty, Y. Kangawa, A. Kusaba, K. Shiraishi, S. Krukowski, M. Bockowski, K. Kakimoto, H. Amano, *Appl. Phys. Lett.* **2017**, *111*, 141602.

© 2019 The Authors. Published by WILEY-VCH Verlag GmbH & Co. KGaA, Weinheim

[21] K. Irmscher, C. Hartmann, C. Guguschev, M. Pietsch, J. Wollweber, M. Bickermann, *J. Appl. Phys.* **2013**, *114*, 123505.
[22] E. Richter, E. Gridneva, M. Weyers, G. Tränkle, *J. Cryst. Growth* **2016**, *456*, 97.
[23] SIMS was performed at RTG Mikroanalyse GmbH, Schwarzschildstraße 1, 12489 Berlin, Germany.
[24] F. Fewster, N. Andrew, *J. Appl. Crystallogr.* **1995**, *28*, 451.
[25] M. A. Moram, M. E. Vickers, *Rep. Prog. Phys.* **2009**, *72*, 036502.
[26] V. Darakchieva, B. Monemar, A. Usui, M. Saenger, M. Schubert, *J. Cryst. Growth* **2008**, *310*, 959.
[27] R. Chierchia, T. Böttcher, H. Heinke, S. Einfeldt, S. Figge, D. Hommel, *J. Appl. Phys.* **2003**, *93*, 8918.
[28] J. A. Freitas, J. C. Culbertson, E. R. Glaser, E. Richter, M. Weyers, A. C. Oliveira, V. K. Garg, *J. Cryst. Growth* **2018**, *500*, 111.
[29] M. A. Reshchikov, J. D. McNamara, H. Helava, A. Usikov, Y. Makarov, *Sci. Rep.* **2018**, *8*, 8091.
[30] S. Ito, H. Kobayashi, K. Araki, K. Suzuki, N. Sawaki, K. Yamashita, Y. Honda, H. Amano, *J. Cryst. Growth* **2015**, *414*, 56.
[31] K. Irmscher, I. Gamov, E. Nowak, G. Gärtner, F. Zimmermann, F. C. Beyer, E. Richter, M. Weyers, G. Tränkle, *Appl. Phys. Lett.* **2018**, *113*, 262101.
[32] M. Hao, S. Mahanty, R. S. Qhalid Fareed, S. Tottori, K. Nishino, S. Sakai, *Appl. Phys. Lett.* **1999**, *74*, 2788.
[33] Y. Xu, X. Yang, P. Zhang, X. Cao, Y. Chen, S. Guo, S. Wu, J. Zhang, Y. Feng, F. Xu, X. Wang, W. Ge, B. Shen, *Appl. Phys. Express* **2019**, *12*, 061002.
[34] T. Tsuchiya, T. Kitatani, A. Terano, K. Mochizuki, *Jpn. J. Appl. Phys.* **2015**, *54*, 035502.

© 2019 The Authors. Published by WILEY-VCH Verlag GmbH & Co. KGaA, Weinheim